

# **Random Flow Generation of Atmospheric Boundary Layer for Large Eddy Simulation Inflow Conditions**

**Yi-Chao Li, Chii-Ming Cheng, Cheng-hsin Chang**

Tamkang University, Wind Engineering Research Center  
151 Ying-Chuan Road, Tamsui Dist., New Taipei City, Taiwan  
liyichao223@gmail.com; cmcheng@mail.tku.edu.tw; cc527330@mail.tku.edu.tw

**Fuh-Min Fang**

National Chung Hsing University, Department of Civil Engineering  
250 Kuo Kuang Rd., Taichung 402, Taiwan R.O.C.  
fmfang@nchu.edu.tw

**Abstract** –To generate the suitable atmospheric boundary layer inlet for large eddy simulation, one of the most important techniques of computational wind engineering, the MDSRFG (modified discretizing and synthesizing random flow generation) was selected to numerically generate the inhomogeneous and anisotropic turbulence boundary layer in this paper. A weakly-compressible-flow method along with the large eddy simulation (LES) was utilized to reproduce the unsteady flow field. Parameters, such as mean wind speeds, turbulence intensities and turbulence integral scales from fully-developed turbulent boundary layer flow were provided by well-established wind tunnel tests. Furthermore, coherence between any two fluctuating wind speeds was taken into account for a more compact simulation of inflow. It was indicated that the method works well as atmospheric boundary layer generator by comparing the characteristics of mean wind speed profiles, turbulence intensity profiles and power spectra at the centerline of several positions along longitudinal direction from wind tunnel tests.

**Keywords:** computation fluid dynamic, turbulence boundary layer, large eddy simulation

## **1. Introduction**

Reproduction of the reliable atmospheric boundary layer flow field is one of the most important issues in computational wind engineering. An appropriate turbulence inlet can not only maintain the mean wind speed and the turbulence characteristics to the downstream, but also generate reliable wind force on structures. Therefore, simulation of a suitable atmospheric boundary layer inlet is one of the most important works of the computational techniques. To successfully validate this technique, The discretizing and synthesizing random flow generation (DSRFG) method, a improving inflow turbulence generation method developed by Huang et al. (2010), is adopted to produce an inlet fluctuating velocity field that meet specific spectrum. Castro et al. (2011) modified the DSRFG to MDSRFG by preserving the statistical quantities at the inlet part of the computation domain and keeping independence of number of points for simulating target spectrum. However, few studies investigated and successfully maintained statistical quantities of the turbulence boundary layer from inlet to the downstream of computation domain. There are still some technical and theoretical problems need to be overcome.

The aim of this study is to generate a suitable inlet condition of 3 typical categories of atmospheric terrains for LES simulation and to evaluate the time and spatial correlation as parameters. The invariant turbulence intensity profile and wind speed spectra in the alongwind direction are examined to ensure successful reproduction of the simulated field from the upstream distance to the testing object.

## 2. Method

### 2. 1. Numerical Method

To simulate the unsteady flow field, a weakly-compressible-flow method (Song and Yuan, 1988) along with a sub-grid scale turbulence model (Smagorinsky, 1963) is employed, the continuity and momentum equations are

$$\frac{\partial p}{\partial t} + \nabla \cdot (k\vec{V}) = 0 \quad (1)$$

$$\frac{\partial \vec{V}}{\partial t} + \vec{V} \cdot \nabla \vec{V} = -\nabla \frac{p}{\rho} + \nabla \cdot [(\nu + \nu_t) \nabla \vec{V}] \quad (2)$$

where  $p$ ,  $\vec{V}$  and  $t$  denote respectively pressure, velocity and time;  $k$  is the bulk modulus of elasticity of air;  $\nu$  and  $\nu_t$  are respectively the laminar and turbulent viscosities. The turbulent viscosity ( $\nu_t$ ) is determined based on a subgrid-scale turbulence model as

$$\nu_t = C_s \Delta^2 \left( \frac{S_{ij}^2}{2} \right)^{0.5} \quad (3)$$

where  $C_s = 0.1$  is the Smagorinsky coefficient;  $\Delta$  denotes the characteristic length of the computational grid and  $S_{ij} = (\partial u_j / \partial x_i + \partial u_i / \partial x_j)$ .

A finite-volume method is adopted to calculate and then update the fluxes within each elapsed time based on an explicit predictor-corrector scheme (MacCormack, 1969). During the computation process, the time increment is limited by the Courant-Friedrich-Lewy criterion (Courant et al., 1967).

### 2. 2. Boundary Conditions

Appropriate values of pressures and velocities are specified at exterior cells (or phantom cells) to reflect the correct physical nature of the boundaries. The ground surface condition is assumed no-slip. The top, both sides and downstream boundaries are assumed zero-gradient conditions (in the directions normal to the boundaries). The fluctuating velocity inlet of upstream boundary condition is generated by the MDSRFG method. The inhomogeneous anisotropic turbulent conditions of the atmospheric boundary are created in this study.

### 2. 2. Synthesizing Method

Derivation of the MDSRFG method and associated validation researches are given by Castro et al. (2011). A brief formulation of the method is presented as below.

$$u(x, t) = \sum_{m=1}^M \sum_{n=1}^N \left[ a_i^{m,n} \cos \left( \tilde{k}_j^{m,n} \tilde{x}_j + \omega_{m,n} \frac{t}{\tau_0} \right) + b_i^{m,n} \sin \left( \tilde{k}_j^{m,n} \tilde{x}_j + \omega_{m,n} \frac{t}{\tau_0} \right) \right] \quad (4)$$

with  $\omega_{m,n} \in N(0, 2\pi f_m)$ ,  $\tilde{x} = x/L_s$  and  $L_s = \theta_1 \sqrt{L_u^2 + L_v^2 + L_w^2}$  is the scaling factor for spatial correlation.  $\tau_0 = \theta_2 L_s / \bar{U}$  is a parameter introduced to allow some control over the time correlation. The

wave number vector  $\tilde{k}^{m,n} = k^{m,n} / k_0$  is the three dimensional distribution on the sphere of inhomogeneous and anisotropic turbulence.

The factors  $a_i^{m,n}$  and  $b_i^{m,n}$  defines the distribution of the three dimensional energy spectrum  $E_i(k_m)$  in each of spatial coordinate axes which are in turn functions of space wave number  $k^{m,n}$ . The distribution of  $k^{m,n}$  is anisotropic on the surface of a sphere and the energy is non-uniformly distributed in the space,  $a_i^{m,n}$  and  $b_i^{m,n}$  have to be aligned with the energy spectrum along a principal direction and then the distribution of  $k^{m,n}$  can be remapped on the surface of the sphere. Where  $a_i^{m,n}$  and  $b_i^{m,n}$  are determined blow:

$$a_i^{m,n} = \text{sign}(r_i^{m,n}) \sqrt{\frac{4c_i}{N} E_i(k_m) \Delta k_m \frac{(r_i^{m,n})^2}{1 + (r_i^{m,n})^2}} \quad (5)$$

$$b_i^{m,n} = \text{sign}(r_i^{m,n}) \sqrt{\frac{4c_i}{N} E_i(k_m) \Delta k_m \frac{1}{1 + (r_i^{m,n})^2}} \quad (6)$$

where  $r_i^{m,n}$  is a three dimensional normal distributed random number with  $\mu_r = 0$  and  $\sigma_r = 1$ .  $c_i = 0.5\bar{U}$  and  $\bar{U}$  is the mean wind speed. Once the target  $a_i^{m,n}$  and  $b_i^{m,n}$  are obtained, the distribution of  $k^{m,n}$  can be remapped on the sphere according to the following equations:

$$a^{m,n} \cdot k^{m,n} = 0 \quad (7)$$

$$b^{m,n} \cdot k^{m,n} = 0 \quad (8)$$

$$|k^{m,n}| = k_m \quad (9)$$

The inhomogeneous anisotropic turbulent conditions of the suburban terrain field were created in this study. The spectra of the three principal velocity components are described by von Kármán models, i.e.,

$$S_u(f) = \frac{4(I_u \bar{U})^2 (L_u / \bar{U})}{[1 + 70.8(fL_u / \bar{U})^2]^{5/6}} \quad (10)$$

$$S_v(f) = \frac{4(I_v \bar{U})^2 (L_v / \bar{U}) [1 + 188.4(2fL_v / \bar{U})^2]}{[1 + 70.8(2fL_v / \bar{U})^2]^{11/6}} \quad (11)$$

$$S_w(f) = \frac{4(I_w \bar{U})^2 (L_w / \bar{U}) [1 + 188.4(2fL_w / \bar{U})^2]}{[1 + 70.8(2fL_w / \bar{U})^2]^{11/6}} \quad (12)$$

where  $I_u$ ,  $I_v$ ,  $I_w$  and  $L_u$ ,  $L_v$ ,  $L_w$  are turbulence intensity and length scale in 3 principle direction respectively.

### 2. 3. Computation Domain and Meshes

In this research, an open terrain model is established to investigate the turbulence variation along the longitudinal direction, and the inflow turbulence is generated by MDSRFG method. The longitudinal (x), horizontal(y), and vertical (z) lengths of computational domain are 15 m, 2 m and 1.25 m respectively. In consideration of computational resource and efficiency, the first point near the wall surface of the domain is set to be 0.005 m, which is also applied at inflow due to drastic change in the flow velocity. The total computational grid points are  $209 \times 101 \times 101$ .

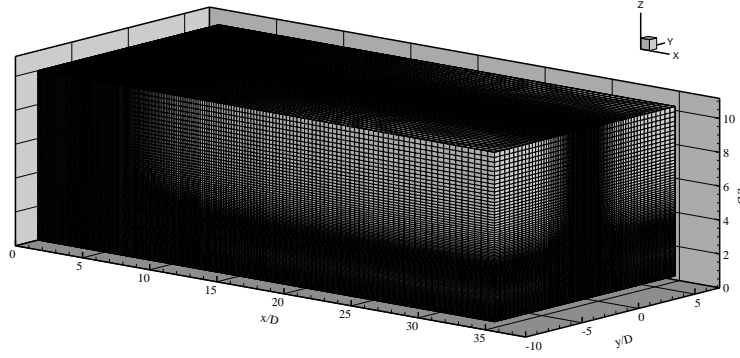


Fig. 1. Computational grid system

### 3. Results

Before synthesizing the instantaneous wind speed of the inlet, there are some preliminary. All the prescribed parameters of longitudinal wind profiles are obtained from TKU BL1 wind tunnel experiments. The mean wind speed profile is set to follow the power law  $u(z) = u_\delta \left(\frac{z}{\delta}\right)^\alpha$ .  $\delta$  is boundary layer thickness,  $u_\delta$  is the velocity of freestream. The u-component turbulence intensity ( $I_u$ ) profile and length scale ( $L_u$ ) profile are regressed into the power law form. The experimental equations of velocity profiles by curve-fitted and the corresponding parameters are shown in Table 1. Because of the lack of v- and w-component of turbulence intensity and length scale, the assumption of the turbulence intensity is adopted in the other two directions, as  $I_v = 0.75I_u$  and  $I_w = 0.5I_u$  respectively.  $L_v$  and  $L_w$  are both assumed as  $0.5L_u$  (ESDU85020, 1985; Farrell et al., 1999).

Table. 1. Parameters of inlet velocity profiles

	T-A(urban)	T-B(suburban)	T-C(open)
$\delta$ (m)	1.25	1	0.75
$\alpha$	0.32	0.25	0.15
$I_u$	$0.35-0.28(z/\delta)^{0.42}$	$0.3-0.26(z/\delta)^{0.35}$	$0.25-0.22(z/\delta)^{0.25}$
$L_u$ (m)	$(z/\delta)^{0.32}$	$0.78(z/\delta)^{0.25}$	$0.5(z/\delta)^{0.15}$

Before synthesizing the wind speed of the inlet, an important work is to determine the appropriate spatial parameter ( $\theta_1$ ) and the time parameter ( $\theta_2$ ).  $\theta_1$  dominates the scaling factor, influences the spatial and time correlation. Since the turbulence boundary layer spectra vary significantly along the vertical direction, to determine  $\theta_1$ , a theoretical equation for reference, the spatial coherence proposed by Davenport (1968), is adopted to be the target function as:

$$Coh = e^{-\hat{f}}, \hat{f} = \frac{n[C_z^2(z_1 - z_2)^2 + C_y^2(y_1 - y_2)^2]^{1/2}}{0.5[U(z_1) + U(z_2)]} \quad (13)$$

where  $y_1, y_2, z_1, z_2$  are the coordinate on y-z plane.  $C_z$  and  $C_y$  are the exponential decay coefficient in the horizontal and vertical direction respectively.  $C_z=10$  and  $C_y=16$  are addressed by Davenport(1968), which consist with the results of TKU BL1. In the boundary layer flow field, the main variation of turbulence intensity and turbulence integral length scale profile are all along the vertical direction, therefore the adjustment of  $\theta_1$  is based on fitting the vertical coherences to correspond the theoretical function.  $\theta_2$  is the parameter introduced to allow for some control over the auto-correlation, therefore  $\theta_2$  can adjust the turbulence integral length scale to correspond original setup. All MDSRFG parameters related to the spatial correlation and time correlation for all testing terrains are listed in Table 2.

Table 2. Parameters of MDSRFG method

	N	M	$\theta_1$	$\theta_2$
<b>T-A</b>	100	2500	10	0.3
<b>T-B</b>	100	2500	5	0.5
<b>T-C</b>	100	2500	5	0.5

Comparing the results show in Fig 2, the mean velocity profiles of u-component vary along x-direction from the inlet to the downstream (1 m). All profiles of 3 terrains at the inlet consistence with the target which obeys the power law. The velocity profiles vary indistinct even to the downstream in all terrains.

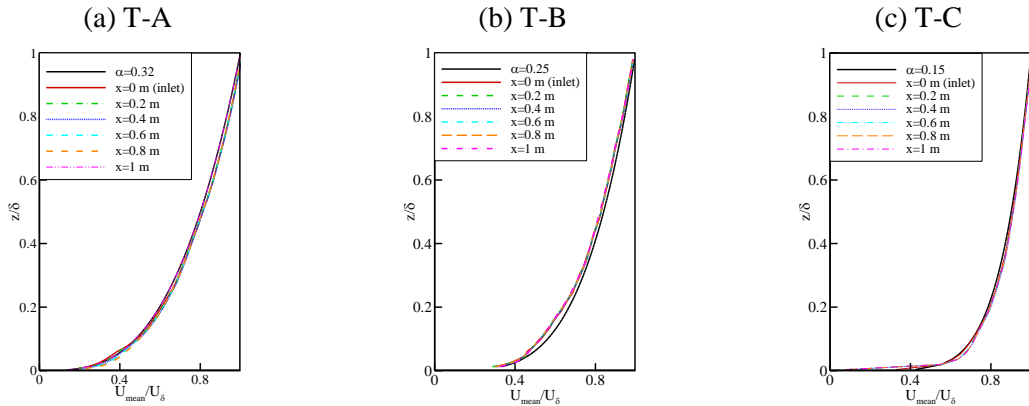


Fig. 2. Comparisons of mean velocity with varying distances along x-direction

The comparisons of u-component turbulence intensity  $I_u$  along x-direction are shown in Fig. 3. Basically, the inlet profiles ( $x=0$  m) synthesized by MDSRFG correspond with the target profiles. The profiles of T-B maintain the turbulence energy to the downstream. The turbulence intensity of T-A and T-C decays near the ground while  $x>0$ . The maximum  $I_u$  decay of T-A and T-C is about 20 %.

Fig. 4 presents the comparisons of v-component turbulence intensity ( $I_v$ ) along x-direction. The results show that  $I_v$  profiles at inlet ( $x=0$  m) have good agreement with the targets in all categories of the terrains. While  $x>0$ , the profiles also fit well to the targets.

The results of w-component turbulence intensity  $I_w$  are shown in Fig. 5. In this study, the assumption  $I_w = 0.5I_u$  is used. In fact, the vertical vortex is depressed by the wall boundary, the turbulence should tend to zero near that wall. Therefore, the turbulence energy is depressed by the wall boundary at first grid

above the wall boundary while  $x > 0$ , the setting energy couldn't be maintained.  $I_w$  trends to the target profiles while the position trends to the upper level.

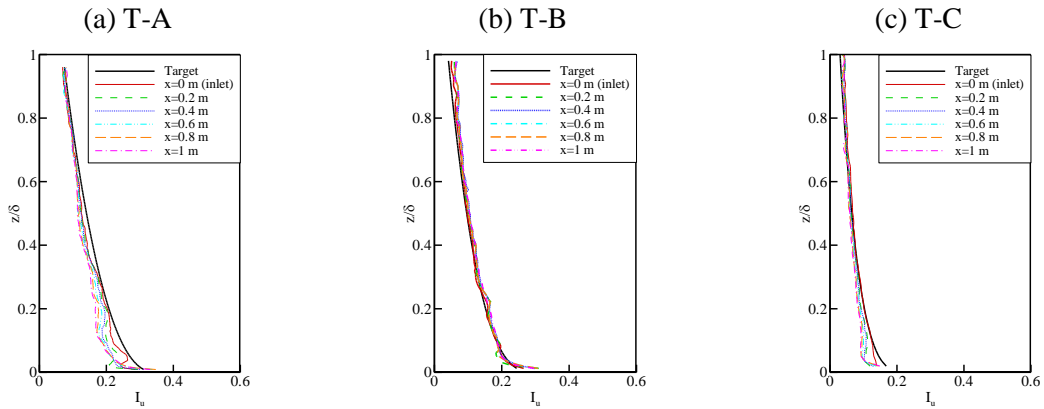


Fig. 3. Comparisons of u-component turbulence intensity with varying distances along x-direction

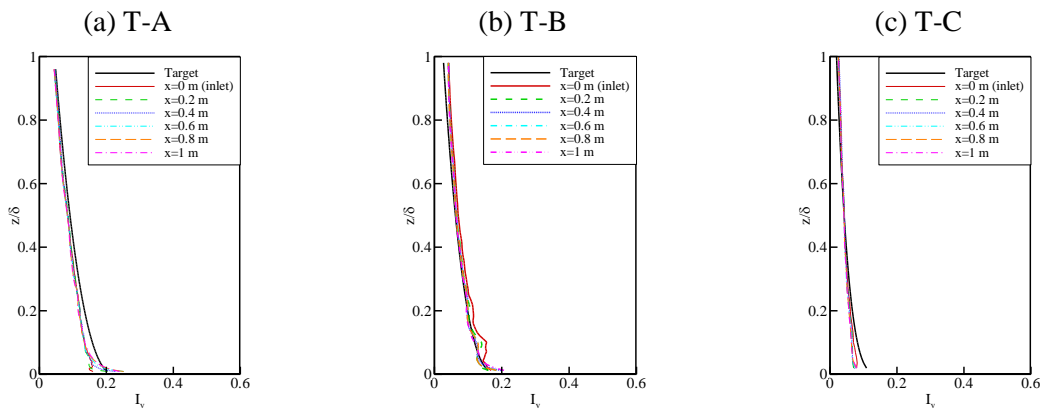


Fig. 4. Comparisons of v-component turbulence intensity with varying distances along x-direction

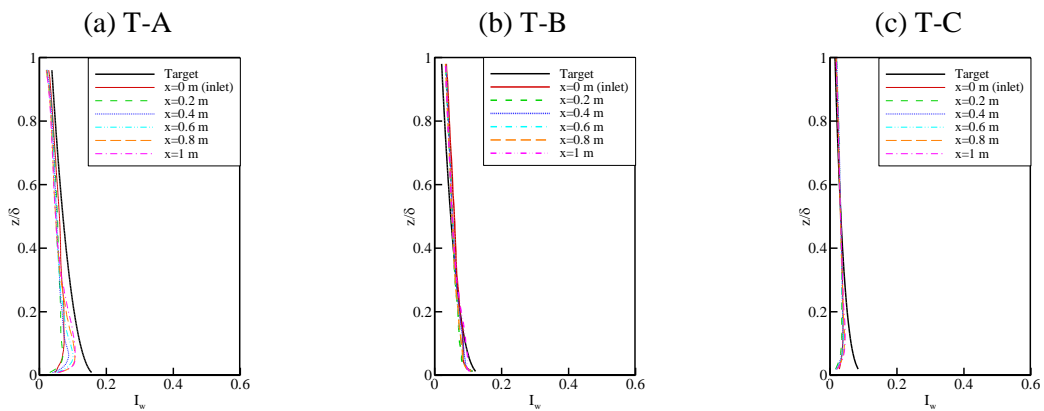


Fig. 5. Comparisons of w-component turbulence intensity with varying distances along x-direction

Overall, a well statistic characteristic is obtained by LES using MDSRFG to synthesize anisotropic velocity inlet. The wind speed profiles of T-B have better agreement then the other two categories of terrains. The wind spectrum of 3 directions at  $z/\delta = 0.25$  are presented in Fig. 6. The results show that the anisotropic spectrum at inlet fairly agree with the targets (von Kármán models). Although the turbulence energy decreases above 25 Hz, the main turbulence energy is clearly described below 25 Hz. The

behaviour of decreasing turbulence energy might be due to the scale of grid is larger than the corresponding scale of turbulence vortex. It should can be improved by adopting finer grid system.

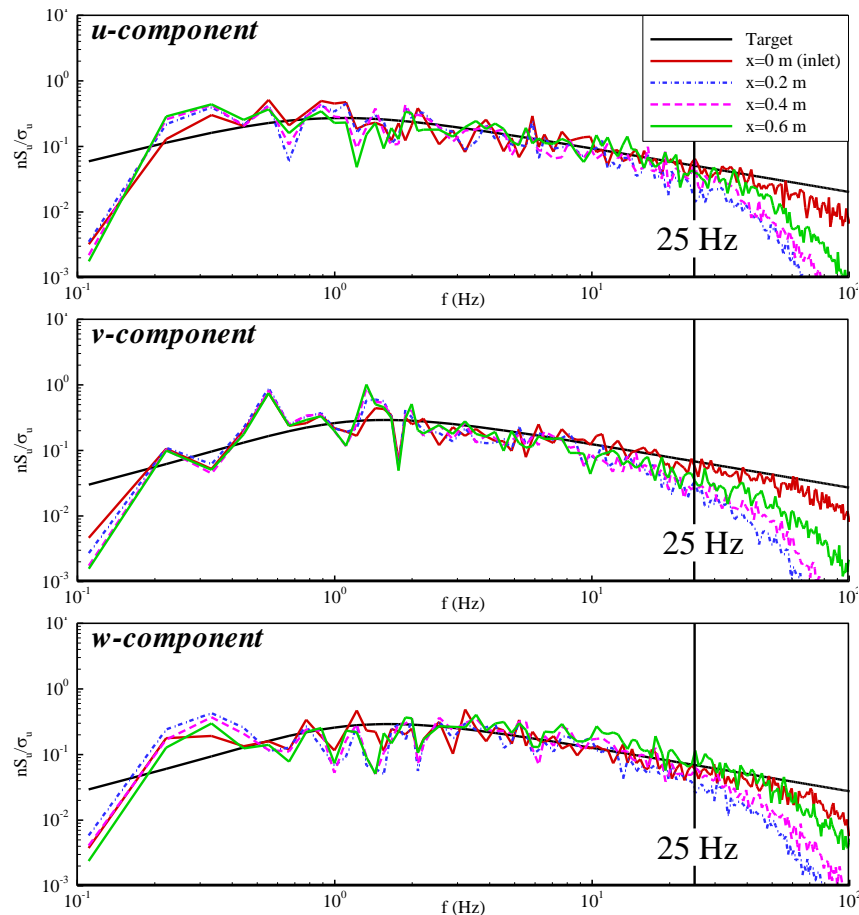


Fig. 6. Comparisons of wind spectrum in 3 direction

#### 4. Conclusion

In this research, the MDSRFG is adopted to generate the inlet boundary condition of 3 typical categories of terrain flow fields for Large-Eddy simulation. The mean wind speed profile, turbulence intensity profiles and power spectra of velocity fluctuations of simulation results fit fairly well to targets. The parameters of spatial and time correlations are adjusted by wind tunnel results and theoretical equations to prove that the MDSRFG method can be an effective numerical tool for generating a spatially correlated atmospheric boundary layer flow field. However, the decay of T-A and T-C turbulent energy at high frequencies is more than the decays of T-B. It may can be improved by adopting finer grid point, or a suitable inflow profile of turbulent intensity and length scale.

#### References

- Castro, H. G., Paz, R. R., & Sonzogni, V. E. (2011). Generation of Turbulence Inlet Velocity Conditions for Large Eddy Simulation. *Mecánica Computacional*, XXX, 2275–2288.
- Courant, R., Friedrich, K., & Lewy, H. (1967). On The Partial Differential Equations Of Mathematical Physics. *IBM Journal*, 11(2), 215-234.
- Davenport, A. G. (1968), The Dependence Of Wind Load Upon Meteorological Parameter. *In Proceedings of the International Research Seminar on Wind Effects on Buildings and Structures*, University of Toronto Press, Toronto, 19-82.

- Engineering Sciences Data Unit, (1985). Characteristics Of Atmospheric Turbulence Near The Ground, *Data Item 85020*, ESDU International Ltd, London.
- Farell, C., & Iyengar, K.S., (1999). Experiments On The Wind Tunnel Simulation Of Atmospheric Boundary Layers. *Journal of Wind Engineering and Industrial Aerodynamics*, 79, 11-35.
- Huang, S. H., Li, Q. S., & Wu, J. R. (2010). A General Inflow Turbulence Generator for Large Eddy Simulation. *Journal of Wind Engineering and Industrial Aerodynamic*, 98, 600-617.
- Li, Y. C., Cheng, C. M., Fang, F. M., Chang, C. H., & Lo, Y.L. (2013). Generation of Suburban Terrain Inflow Conditions for Large Eddy Simulations. *The 8th Asia-Pacific Conference on Wind Engineering*, Chennai, India.
- Li, Y. C., Cheng, C. M., Fang, F. M., Chang, C. H., & Lo, Y.L. (2014). Simulation Of Turbulent Flows Around A Prism In Suburban Terrain Inflow Based On Random Flow Generation Method. *The 6th International Symposium on Computational Wind Engineering*, Hamburg, Germany.
- MacCormack, R. (1969). The Effect Of Viscosity In Hyper-Velocity Impact Cratering. *AIAA paper*, 69-354.
- Smagorinsky, J. (1963). General Circulation Experiments With Primitive Equations. *Month Weather Review*, 91(3), 99-164.
- Sminov, A., Shi, S., & Celik, I. (2001). Random Flow Generation Technique for Large Eddy Simulation and Particle-Dynamics Modeling. *Journal of Fluids Engineering*, 123, 359-371.
- Song, C., & Yuan, M. (1988). A Weakly Compressible Flow Model And Rapid Convergence Methods. *Journal of Fluids Engineering*, 110(4), 441-455.